MOLECULAR CARCINOGENESIS 55:193–208 (2016)

Tissue Inhibitor of Matrix Metalloproteinase-1 Expression in Colorectal Cancer Liver Metastases is Associated With Vascular Structures

Martin Illemann,[1,2]* Rikke Helene Løvendahl Eefsen,[1,2,3] Nigel Charles Bird,[4] Ali Majeed,[4] Kell Osterlind,[3] Ole Didrik Laerum,[1,2] Warner Alpízar-Alpízar,[1,2,5] Ida Katrine Lund,[1,2] and Gunilla Høyer-Hansen[1,2]

[1]*The Finsen Laboratory, Rigshospitalet, Copenhagen, Denmark*
[2]*Biotech Research and Innovation Center (BRIC), University of Copenhagen, Copenhagen, Denmark*
[3]*Department of Oncology, Rigshospitalet, Copenhagen, Denmark*
[4]*Academic Surgical Unit, University of Sheffield, Sheffield, England*
[5]*Center for Research on Microscopic Structures, University of Costa Rica, San José, Costa Rica*

Metastatic growth by colorectal cancer cells in the liver requires the ability of the cancer cells to interact with the new microenvironment. This interaction results in three histological growth patterns of liver metastases: desmoplastic, pushing, and replacement. In primary colorectal cancer several proteases, involved in the degradation of extracellular matrix components, are up-regulated. In liver metastases, their expression is growth pattern dependent. Tissue inhibitor of matrix metalloproteinase-1 (TIMP-1) is a strong prognostic marker in plasma from colorectal cancer patients, with significant higher levels in patients with metastatic disease. We therefore wanted to determine the expression pattern of TIMP-1 in primary colorectal cancers and their matching liver metastases. TIMP-1 mRNA was primarily seen in α-smooth-muscle actin (α-SMA)-positive cells. In all primary tumors and liver metastases with desmoplastic growth pattern, TIMP-1 mRNA was primarily found in α-SMA-positive myofibroblasts located at the invasive front. Some α-SMA-positive cells with TIMP-1 mRNA were located adjacent to CD34-positive endothelial cells, identifying them as pericytes. This indicates that TIMP-1 in primary tumors and liver metastases with desmoplastic growth pattern has dual functions; being an MMP-inhibitor at the cancer periphery and involved in tumor-induced angiogenesis in the pericytes. In the liver metastases with pushing or replacement growth patterns, TIMP-1 was primarily expressed by activated hepatic stellate cells at the metastasis/liver parenchyma interface. These cells were located adjacent to CD34-positive endothelial cells, suggesting a function in tumor-induced angiogenesis. We therefore conclude that TIMP-1 expression is growth pattern dependent in colorectal cancer liver metastases.

Key words: TIMP-1; hepatic metastasis; desmoplasia; angiogenesis; histology

INTRODUCTION

Colorectal adenocarcinomas usually metastasize to the liver, in which the interaction between the metastatic cancer cells and the liver microenvironment gives rise to metastases that can grow in three different morphologies [1,2]. These are: *desmoplastic*; where the cancer cells are separated from the liver parenchyma by a dense zone of desmoplasia containing stromal cells such as macrophages and fibroblasts; *pushing*, where the liver plates are compressed at the metastasis/liver parenchyma interface; *replacement*, where the tumor cells infiltrate the liver cell plates, replacing the hepatocytes [1,2]. Importantly, multiple colorectal cancer liver metastases resected from chemonaive patients tend to have one predominant growth morphology [3]. Metastases with different growth patterns differ in angiogenesis with the highest activity in those with pushing growth pattern [1,3,4].

In vitro as well as in vivo studies have shown that cancer invasion and metastasis are associated with proteolytic degradation of the extracellular matrix [5–7]. We have earlier reported that metastases with a desmoplastic growth pattern showed intense

[The copyright line for this article was changed in January 2016 after original online publication.]

Abbreviations: mAb, monoclonal antibody; MMP, matrix metalloproteinase; PAI-1, plasminogen activator inhibitor-1; pAb, polyclonal antibody; α-SMA, α-smooth-muscle-actin; TIMP-1, tissue inhibitor of metalloproteinases-1; uPA, urokinase-type plasminogen activator; uPAR, uPA receptor.

Grant sponsor: The Villum Foundation (to MI), The Capital Region of Denmark, Foundation for Health Research (to GHH), Danish Cancer Research Foundation, European Community's Seventh Framework Program FP7/2007-2011 under grant agreement no 201279 (to GHH), Danish Cancer Society (to WAA), and The Lundbeck Foundation (to IKL)

*Correspondence to: Martin Illemann, The Finsen Laboratory, Rigshospitalet, Ole Maaløes Vej 5 3rd floor, DK-2200 Copenhagen N, Denmark.

Received 10 July 2014; Revised 30 October 2014; Accepted 26 November 2014

DOI 10.1002/mc.22269

Published online 15 January 2015 in Wiley Online Library (wileyonlinelibrary.com).

expression of urokinase-type plasminogen activator (uPA), its cellular receptor (uPAR), and the uPA inhibitor (PAI-1) primarily in stromal cells located within the desmoplastic zone [8]. In metastases with the pushing growth pattern, uPA and uPAR were only present in necrotic areas within the liver metastases, whereas PAI-1 was found in hepatocytes and activated hepatic stellate cells at the periphery of the metastases [8]. In metastases of the replacement growth pattern uPAR was distributed in a pattern similar to that found in liver metastases with the pushing growth pattern [3]. Intriguingly, such differences were not observed in the primary colorectal cancer where, uPA, uPAR and PAI-1 were expressed mainly by stromal cells at the invasive front of all primary tumors [8]. We have also localized matrix metalloproteinase 9 (MMP-9) in primary and metastatic colorectal cancer [9]. MMP-9 was only up-regulated at the invasive front of primary colorectal cancer but not in the metastases. These data suggest that the proteolytic mechanisms involved in primary tumor invasion and liver metastasis growth are distinct and may provide insight into the mechanisms underlying the diversity in growth patterns (see Table 1). It is therefore likely, that liver metastases with a desmoplastic growth pattern, as their primary tumors, require the expression of matrix-degrading components in order to grow and invade into the surrounding liver compartments. Such components may not be needed for the expansion/invasion of metastases with pushing and/or replacement growth pattern, as the cancer cells might invade the liver using the cavity of the sinusoids or by direct replacement of the hepatocytes [8].

The enzymatic activity of MMPs in vivo is tightly regulated by tissue inhibitor of metalloproteinases (TIMP), a family of four small (20–29 kDa) extracellular proteins [7]. TIMPs inhibit reversibly the MMPs by binding the zinc-binding site of active MMPs in a 1:1 stoichiometric fashion [7]. The ability to inhibit the various MMPs differs for each TIMP; however, most soluble MMPs can be inhibited by TIMP-1.

TIMP-1 is secreted into the blood and is measurable in healthy donors, but patients with colorectal cancer have significantly higher levels [10]. High levels of TIMP-1 measured by ELISA in preoperative plasma from colorectal cancer patients are associated with short survival [11]. This association was independent of clinical parameters including tumor stage; however, a significantly higher level of TIMP-1 in plasma was found in patients with metastatic (Dukes' D) disease. This implies that TIMP-1 is synthesized in the primary tumor as well as in the metastases.

In colorectal cancer, TIMP-1 mRNA is primarily expressed by tumor associated myofibroblasts at the invasive front of the tumor [12–14] though expression has also been seen in some cancer cells [12]. In colorectal cancer liver metastases TIMP-1 mRNA have been localized to "spindle fibroblast-like stroma cells" [15]. The cellular localization of TIMP-1 has not been described in detail or with regards to the growth patterns.

We have here determined the expression pattern of TIMP-1 in primary colorectal cancer and its matching liver metastasis. TIMP-1 is primarily expressed in α-smooth-muscle-actin (α-SMA)-positive cells in both primary colorectal cancer and in liver metastases regardless of growth pattern. About half of the TIMP-1-positive cells at the invasive front in primary colorectal cancer and at the periphery of liver metastases with desmoplasia are expressed by pericytes, whereas almost all TIMP-1-positive cells in liver metastases with pushing or replacement growth patterns were identified as activated hepatic stellate cells.

MATERIALS AND METHODS

Tissue Samples

Tissue samples from 29 colorectal adenocarcinomas were obtained together with their matching liver metastases (18 synchronous and 11 metachronous) from Royal Hallamshire Hospital (Sheffield, UK). The liver metastases (ranging from 1 to 7 metastases per patient, 1 representative metastasis from each patient was selected for this study) were removed during partial hepatectomy with mean interval of 87 days (range 13–485 days) after the discovery of metastasis. Following surgical resection, ~4 mm-thick tissue specimens were on the same day dissected from the tumor and immediately thereafter fixed in 4% neutral-buffered formalin for 20–24 h at room temperature and then paraffin-embedded. The samples were obtained from a group of patients including 11 women and 18 men in the age interval 36–79 (age at colon and rectum surgery). The liver metastases were collected prospectively from 1997–2003 and are randomly assembled from a data base containing samples from 247 operations all performed by one surgeon (Dr. Ali Majeed). Their use for research had been approved by South Sheffield Research Ethics Committee (STH 14722).

In order to increase the number of liver metastases 10 additional liver metastases of each growth pattern were identified from a patient cohort who underwent liver resection at Rigshospitalet, Copenhagen, Denmark from 2007 to 2011 (Ethical approval from regional ethical committee in Denmark number H-2–2011-045). These metastases were collected from 26 patients (16 synchronous and 10 metachronous). Eight of the patients were women and 18 men and the patients were in the age interval 24–83 at liver surgery. Nineteen of the patients had multiple metastases removed. From 22 of the patients, one metastasis was included and from four of the patients 2 metastases were included.

The metastatic lesions in all liver tissue samples were CK20 positive and CK7 negative confirming that

Table 1. Expression of Proteases and Inhibitors in Primary Colorectal Cancer and Liver Metastases With Different Growth Pattern

		Liver Metastasis (Invasive front)		
Protein	Colon Adenocarcinoma (Invasive front)	Desmoplastic growth pattern	Pushing growth pattern	Replacement growth pattern
TIMP-1*	α-SMA-positive myofibroblasts Pericytes Cancer cells	α-SMA-positive myofibroblasts Pericytes Hepatocytes Cancer cells	Hepatic stellate cells Hepatocytes Cancer cells	Hepatic stellate cells Hepatocytes Cancer cells
MMP-2*	Fibroblasts	Fibroblasts	Not detected	NA
MMP-9**	CD68-positive macrophages Infiltrating neutrophils	Infiltrating neutrophils	Infiltrating neutrophils	NA
uPAR‡	CD68-positive macrophages α-SMA-positive myofibroblasts LN5γ2-positive budding cancer cells Infiltrating neutrophils	CD68-positive macrophages α-SMA-positive myofibroblasts LN5γ2-positive budding cancer cells Infiltrating neutrophils	Infiltrating neutrophils	CD68-positive macrophages Infiltrating neutrophils
uPA†	α-SMA-positive myofibroblasts CD68-positive macrophages LN5γ2-positive budding cancer cells	α-SMA-positive myofibroblasts CD68-positive macrophages LN5γ2-positive budding cancer cells	Not detected	NA
PAI-1*	α-SMA-positive myofibroblasts CD34-positive endothelial cells CD68-positive macrophages	α-SMA-positive myofibroblasts CD34-positive endothelial cells CD68-positive macrophages Hepatocytes	Hepatic stellate cells Hepatocytes	Hepatic stellate cells* Hepatocytes*

Localization studies for TIMP-1, MMP-9, uPAR and PAI-1 has been done with both immunohistochemistry and in in situ hybridizations. For MMP-2 and uPA localization has only been done using in situ hybridizations. NA, not accessed.
*Results from this study.
**Illemann *et al.*, 2006 (ref 9).
†Illemann *et al.*, 2009 (ref 8).
‡Eefsen *et al.*, 2012 (ref 3).

all liver samples were metastasis of colorectal cancer [16]. The growth pattern of the liver metastases were evaluated by staining for reticulin fibers and hematoxylin and eosin as earlier described [3,8].

Antibodies

Monoclonal antibodies (mAb) against TIMP-1 (clone VT7), α-SMA (clone 1A4), CD34 (clone QBEnd10), CD68 (clone PG-M1), CK20 (clone K_s20.8) and CK7 (clone OV-TL) as well as EnVision™ Horseradish Peroxidase Mouse (K4001) EnVisionTM Horseradish Peroxidase Rabbit (K4003) were purchased from Dako (Glostrup, Denmark). The polyclonal antibody (pAb) against PAI-1 has previously been described [17]. Cy3-conjugated goat-anti-mouse IgG and FITC-conjugated goat-anti-rabbit IgG were purchases from Jackson ImmunoResearch (West Grove, PA).

In vitro Transcription and In Situ Hybridization

In vitro transcription and in situ hybridization were performed as previously described [8]. TIMP-1 antisense and sense riboprobes were generated from PCR constructs f104, f105 and f106 [14]. MMP-2 antisense and sense riboprobes were generated from plasmid pCol7201 [14,18]. The ^{35}S-radioactivity concentration of the probes was adjusted by dilution to 500,000 cpm/μl. Each section was prior to the in situ hybridization pre-treated at 98°C at 10 min in TEG-buffer (10 mM Tris, 0.5 mM EGTA, pH 9.0) using a T/T Micromed microwave processor (Milestone, Sorisol, Italy) and the section was developed after exposure to autoradiographic emulsion (ILFORD Imaging, UK Limited, Mobberley, UK) for 7 days at 4°C.

Imunoperoxidase Staining

Three μm thick paraffin sections were used for immunoperoxidase staining. Antigen retrieval was performed at 98°C for 10 min (TIMP-1, CK20 or CK7) or 30 min (PAI-1) in TEG-buffer using a T/T Micromed microwave processor. Endogenous peroxidase activity was blocked by incubation with 1% H_2O_2 for 15 min. The sections were washed in Tris-buffered saline (TBS, 50 mM Tris-HCL, 150 mM NaCl) containing 0.5% Triton X-100 (TBS-T), and then mounted in Shandon racks with immunostaining cover plates (Thermo Shandon, Pittsburgh, PA) for further incubations. The antibodies were diluted in Antibody Diluent with Background-Reducing Components (S3022, Dako, Glostrup, Denmark) to a concentration of 0.23 μg/mL (TIMP-1), 0.48 μg//mL (CK20), 0.65 μg//mL (CK7) or 1.00 μg//mL (PAI-1) and added to the slide and incubated overnight at 4°C. The mAbs was detected with EnVision™ Horseradish Peroxidase Mouse and the pAb was detected with EnVision™ Horseradish Peroxidase Rabbit. Each incubation step was followed by washes in TBS-T. The sections were developed with NovaRed (Vector laboratories, Burlingame, CA) and counterstained in Mayer's hematoxylin, and finally dehydrated and mounted using a Dako Coverslipper.

Combined Immunohistochemistry and In Situ Hybridization

Prior to TIMP-1 in situ hybridization, the sections were under RNase free conditions pre-treated in TEG-buffer as described above. They were then stained for either α-SMA (0.35 μg/mL), CD34 (0.13 μg/mL), CD68 (0.30 μg/mL) or TIMP-1 (0.23 μg/mL), detected with EnVision™ Horseradish Peroxidase Mouse, and developed with diaminobenzidine chromogene (DAB) (Sigma–Aldrich, St. Louis, MO) using protocol previously described [8]. The ^{35}S-labeled TIMP-1 mRNA probes were applied and exposed as described above, thereafter counterstained with Mayer's hematoxylin, dehydrated and mounted with pertex using a Dako CoverSlipper.

TIMP-1 and PAI-1 Double Immunofluorescence

Three μm thick paraffin sections were deparaffinized, pre-treated and mounted on Shandon racks as described above. The TIMP-1 mAb (0.23 μg/mL) was diluted in Antibody Diluent with Background-Reducing Components together with the PAI-1 pAb (0.5 μg/mL) and added to the sections. Incubation was performed overnight at 4°C. The antibodies were detected with Cy3-conjugated goat-anti-mouse (TIMP-1) and FITC-conjugated goat-anti-rabbit (PAI-1) diluted in Antibody Diluent with Background-Reducing Components to a final concentration of 10 μg/mL. The sections were washed in TBS after each incubation step. The sections were finally mounted with ProLong® Gold antifade reagent (Molecular Probes, Eugene, OR).

Confocal Microscopy

A confocal laser scanning microscope equipped with a 488 nm argon laser and a 543 nm HeNe1 laser (LSM 510 META, Carl Zeiss, Jena, Germany) was used for analyzing the double immunofluorescence stained sections. The images were obtained using the λ-mode (pinhole diameter, 136 μm) collecting images from 509 to 595 nm. Emission spectra for FITC- and Cy3-, and auto-fluorescence were used for emission fingerprinting [19].

Cell Culture and Western Blotting

LX-1 and LX-2 were generated by either SV40 T antigen immortalization (LX-1) of primary hepatic stellate cells or spontaneous immortalization of a subline of LX-1, being able to grow under low serum conditions (LX-2) [20]. The cells were grown to confluency in DMEM (Gibco Cat nr 61965–026, Life Technologies, Carlsbad, CA) supplemented with 10% heat-inactivated fetal calf serum and 200 U/mL penicillin and 25 μg/mL of streptomycin and harvested by detachment using a rubber policeman. The

harvested cells were lysed using temperature induced phase separation in Triton X-114 containing buffer (0.1 M Tris-HCl, pH 8.1, 1% Triton X-114, 10 mM EDTA, 10 μg/mL aprotinin and 1 mM phenylmethylsulfonyl fluoride) [21]. The resulting water- and detergent-phases were analyzed by Western blotting for presence of TIMP-1, PAI-1 and α-SMA using the same primary antibodies as for the immunohistochemistry. Water- or detergent-phase from 9.4×10^5 cells was loaded in each lane. The proteins were separated on 4–12% SDS-PAGE and were electroblotted onto polyvinylidene difluoride membranes using the iBlot system (Life Technologies). Recombinant human TIMP-1, used as a reference, was a kind gift from Professor Gillian Murphy, University of Cambridge, UK. Membranes were blocked in TBS containing 5% skimmed milk powder for 1 h at room temperature, before incubation with 2 μg/mL of antibodies against TIMP-1, PAI-1, and α-SMA. Horseradish peroxidase conjugated rabbit anti-mouse IgG (P0161, Dako) diluted 1:1000 in blocking buffer and Horseradish peroxidase conjugated swine anti-rabbit IgG (P0399, Dako) diluted 1:3000 in blocking buffer were used as secondary reagent and incubated for 1 h at room temperature. Luminata™ Forte (Millipore Corporation, Darmstadt, Germany) was used as the ECL detection system for visualization of the bands.

RESULTS

In this study, we examined the expression and localization of TIMP-1 in 29 primary colorectal adenocarcinomas and matching liver metastasis. All liver metastasis tissue samples were stained for reticulin fibers in order to characterize the growth pattern according to Vermeulen et al. [1] and therefore to be able to differentiate our findings according to the growth patterns. Of the 29 liver metastases with paired primaries, 14 (∼48%) showed desmoplastic growth pattern, 14 (∼48%) displayed pushing growth pattern, while 1 (∼4%) exposed replacement growth pattern [3,8,22].

TIMP-1 In Situ Hybridization in Primary Colorectal Adenocarcinoma and Its Matching Liver Metastasis

All 29 paired samples of primary colorectal adenocarcinomas and their matching liver metastases were processed for *in situ* hybridization using two previously employed non-overlapping antisense TIMP-1 ^{35}S-UTP mRNA probes [14]. In all 29 samples of primary colorectal adenocarcinomas, TIMP-1 mRNA was seen primarily in fibroblast-like cells at the tumor periphery and in a pattern similar to that previously described [14] (see Figure 1A, D). TIMP-1 mRNA was also expressed by some cancer cells scattered throughout the tumor tissue (primarily in the tumor core), and in fibroblast-like cells located in the pericolic fat far from the cancer cells (data not shown).

TIMP-1 mRNA was found in all liver metastases. In all the metastases with desmoplastic growth pattern, TIMP-1 mRNA was primarily seen in fibroblast-like cells within the desmoplastic stromal formation (see Figure 1B, E and Figure 2A, C). TIMP-1 mRNA was also seen in a few hepatocytes located at the interface between the desmoplastic zone and the liver parenchyma (see red arrow in Figure 2A, C). In liver metastases with either pushing or replacement growth patterns, TIMP-1 mRNA was primarily seen in spindle-shaped cells located within the sinusoids of the liver as well as in some few hepatocytes located at the metastasis/liver parenchyma interface (see Figure 1C, F, and Figure 2B, D). TIMP-1 mRNA was furthermore found in fibroblast-like cells located in between the cancer glands of the metastasis in all metastases analyzed.

As for the primary colorectal adenocarcinomas, TIMP-1 mRNA was also detected in the cancer cells scattered throughout the tumor tissue in all the metastases (primarily in the metastasis core, data not shown). Interestingly, TIMP-1 mRNA signal was generally stronger in the liver metastases than in the primary colorectal adenocarcinomas (Figure 1A, D versus 1B, E and 1 C, F). Moreover, the TIMP-1 mRNA signal was stronger in liver metastases with a desmoplastic growth pattern than in those with a pushing or a replacement growth patterns. TIMP-1 mRNA was also observed in central parts of the metastases and associated with fibrotic and necrotic areas (data not shown).

In all samples identical TIMP-1 mRNA signals were obtained when using the two non-overlapping probes. The two corresponding sense ^{35}S-UTP mRNA probes included as negative controls did not give rise to any signal (data not shown).

TIMP-1-Immunohistochemistry in Colorectal Cancer Liver Metastases

Adjacent sections from eight representative samples of liver metastases (four with desmoplastic and four with pushing growth pattern) from the cohort with matching primaries were processed either for TIMP-1 in situ hybridization or TIMP-1-immunohistochemistry using a mAb against TIMP-1. The anti-TIMP-1 antibody has previously been validated for use in immunohistochemistry [14]. The TIMP-1 protein was in general confined to the cytoplasm, but the presence of cell surface-bound TIMP-1 cannot be excluded (see Figure 2E, F). The in situ hybridization for TIMP-1 on adjacent sections showed mRNA signal in cells similar to those expressing TIMP-1 protein (see Figure 2).

In the four liver metastases with a desmoplastic growth pattern, TIMP-1-immunoreactivity was seen primarily in fibroblast-like cells located in front of the metastatic lesion and in between the cancer glands (see black arrows in Figure 2E). A few hepatocytes, located at the interface of the desmoplastic stroma formation and the liver parenchyma, were also positive for TIMP-1 (see red arrows in Figure 2E). In

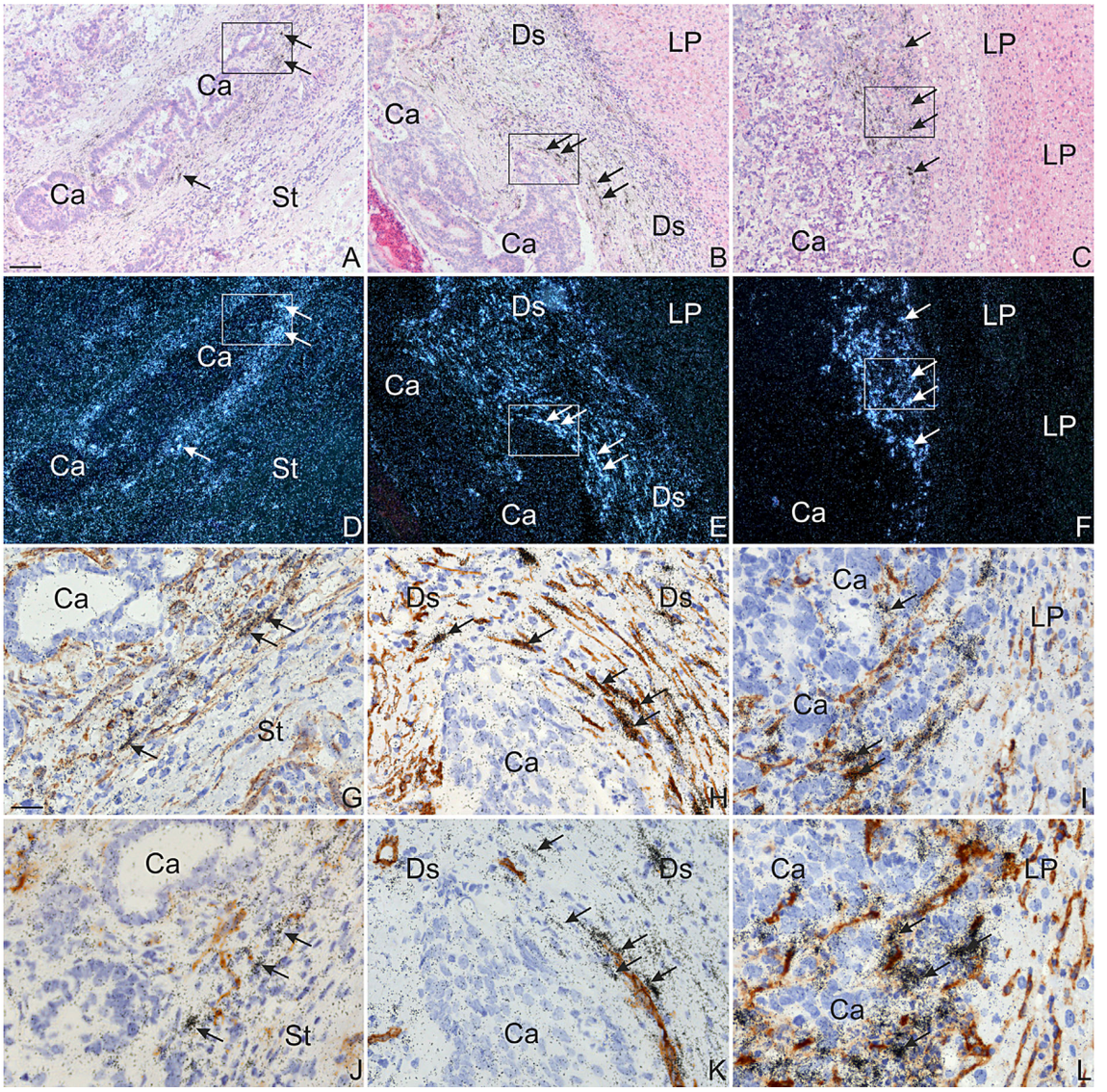

Figure 1. *In situ* hybridization for TIMP-1 mRNA in colon adenocarcinoma and liver metastases. Section from a colon adenocarcinoma (Left Column: A, D, G, J), its liver metastasis with desmoplastic growth pattern (Centre Column: B, E, H, K) and a liver metastases with pushing growth pattern (Right Column. C, F, I, L) were processed for *in situ* hybridization using TIMP-1 mRNA antisense probes (Top Two Rows: A–F) or TIMP-1 mRNA antisense probes combined with immunoperoxidase staining (Bottom Two Rows: G–L) with mAbs for α-SMA (Third Row: G–I) or CD34 (Fourth Row: J–L). The TIMP-1 mRNA probe is visualized as black silver grains in bright-filed illumination (A–C, G–L) and white spots in dark-field illumination (D–F), and the immunoperoxidase staining is detected using DAB (G–L). Loci of particular interest marked with boxes in A–F are showed as close ups in G–L. In all samples, TIMP-1 mRNA is found in stromal fibroblast-like cells at the tumor edge of the cancer/metastasis (indicated with Ca) (arrows in A–F). In the liver metastases, TIMP-1 mRNA is also observed in the stroma in between the cancer glands. Combined immunoperoxidase stained for α-SMA (G–I) or CD34 (J–L) and *in situ* hybridization for TIMP-1 was carried out on adjacent sections from a colon adenocarcinoma, a liver metastasis with desmoplastic growth pattern and a liver metastases with pushing growth pattern. In both colon cancer and liver metastasis with desmoplastic growth pattern, TIMP-1 mRNA was in general found expressed by α-SMA-positive myofibroblasts (arrows in G–H). These TIMP-1 mRNA positive myofibroblasts are often located neighboring CD34-positive endothelial cells (arrows in J–K). TIMP-1 mRNA is in liver metastasis with pushing growth pattern seen in presumably α-SMA-positive hepatic stellate cells (arrows in I). TIMP-1 mRNA was not detected in CD34-positive cells (arrows in L). Bars, ~100 μm (A–F) and ~25 μm (G–L).

contrast, in the four liver metastases with a pushing growth pattern, TIMP-1-immunoreactivity was primarily seen in spindle-shaped cells located at the edge of the tumor as well as in between the tumor glands (see black arrows in Figure 2F) and in some hepatocytes located at the metastasis/liver parenchyma interface (see red arrows in Figure 2F) as well as in hepatocytes located at a distance to the metastasis/liver parenchyma interface (see green arrows in Figure 2F). In all eight samples, TIMP-1 protein was also observed in fibroblast-like cells located in central parts of the metastasis in areas with fibrosis and/or

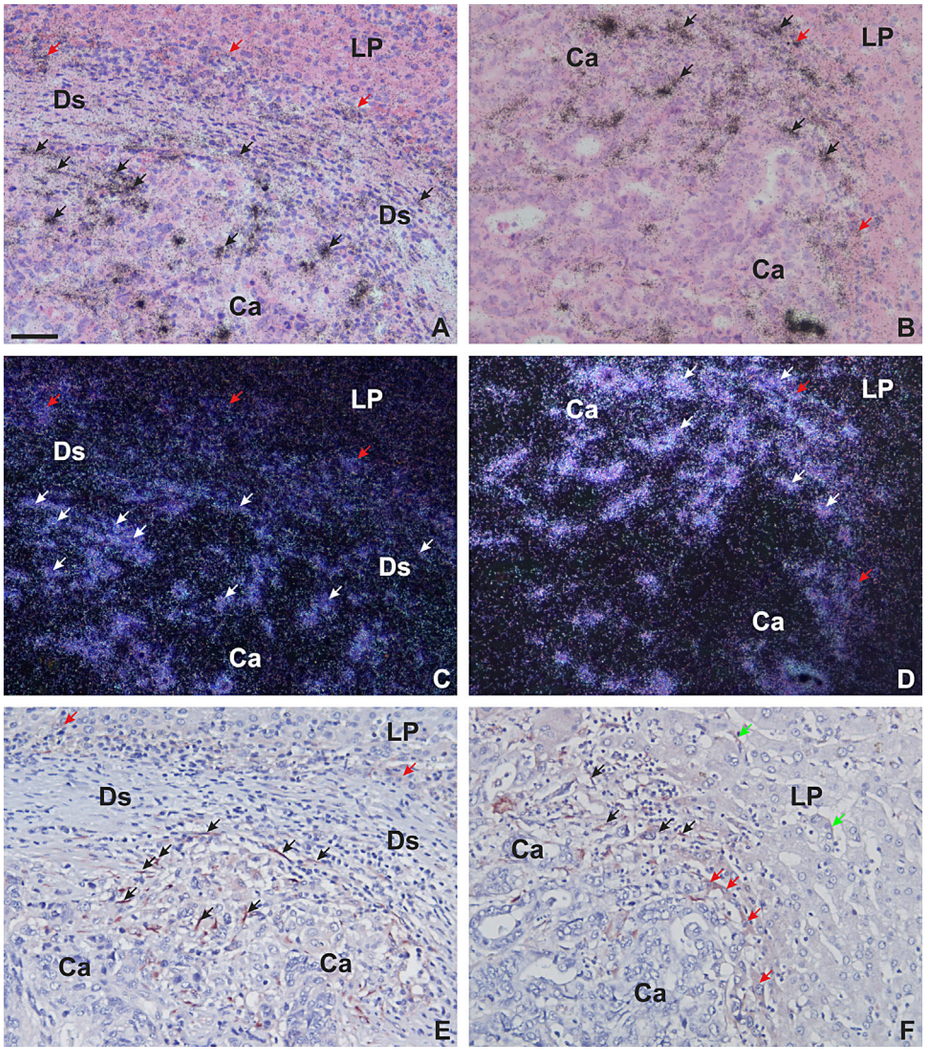

Figure 2. *In situ* hybridization and immunohistochemistry for TIMP-1 mRNA and protein in liver metastases. Adjacent sections from a liver metastasis with desmoplastic growth pattern (Left Column, A, C, E) and a liver metastasis with pushing growth pattern (Right Column, B, D, F) were processed for *in situ* hybridization using TIMP-1 mRNA antisense probes (Two Upper Rows, A–D) or immunoperoxidase staining using a mAb against TIMP-1 (Lower Row, E, F). The TIMP-1 mRNA probe is visualized as black silver grains in bright-field illumination (A, B) and white spots in dark-field illumination (C–D) and the TIMP-1-immunoperoxidase stainings are developed with NovaRed (E, F). In liver metastases with desmoplastic growth pattern, TIMP-1-immunoreactivity is primarily observed in myofibroblasts located within the desmoplastic zone (indicated with DS) near the metastatic cancer cells (black arrows in E). In liver metastases with pushing growth pattern, TIMP-1-immunoreactivity is observed primarily in activated hepatic stellate cells (black arrows in F). TIMP-1-immunoreactivity is also observed in few hepatocytes located at the rim of the metastatic zone, either at the desmoplastic/liver parenchyma interface (red arrows in E) or at the metastasis/liver parenchyma (indicated with LP) interface (red arrows in F). TIMP-1 was also seen in some few hepatic stellate cells located a short distance from the metastasis (green arrows in F). TIMP-1 mRNA was on adjacent sections found in cells similar to those positive for TIMP-1-immunoreactivity (arrows in A–D). TIMP-1 mRNA is also observed in some hepatocytes at the rim of the metastatic zone (red arrows in B and D). Bar in A, ~50 μm.

necrosis (data not shown), and in some cancer cells scattered throughout the tumor tissue (primarily in the metastatic core, data not shown).

Identification of the TIMP-1 mRNA Expressing Cells by Combined Immunohistochemistry and In Situ Hybridization

Eight representative samples of primary colorectal adenocarcinoma and their matching liver metastases, of which four had a desmoplastic growth pattern, and four had a pushing growth pattern were chosen for further analysis in order to identify the cells producing TIMP-1 mRNA. A combined immunohistochemistry and in situ hybridization was used with mAbs against α-SMA (detection of myofibroblasts and pericytes), CD34 (detection of endothelial cells) or CD68 (for detection of monocytes and macrophages), and TIMP-1 mRNA antisense probes.

In all eight representative samples of primary colorectal adenocarcinoma and in the four liver

metastases with desmoplastic growth pattern, TIMP-1 mRNA was found primarily in α-SMA-positive myofibroblasts located at the periphery of the cancer (primary tumors) or within the desmoplastic stroma formation (liver metastases), but also in between the cancer glands (see Figure 1G, H). In both primary colorectal cancer and the liver metastases with desmoplastic growth pattern, a fraction (∼50%) of the TIMP-1 mRNA expressing α-SMA-positive cells were located adjacent to CD34-positive endothelial cells, indicating that these TIMP-1-expressing cells were pericytes (see Figure 1J, K). This demonstrates that the main sites of synthesis of TIMP-1 protein in primary colorectal cancer and the liver metastases with desmoplastic growth pattern are α-SMA-positive myofibroblasts and pericytes. In all four liver metastases with pushing growth pattern, TIMP-1 mRNA was found in α-SMA-positive cells located within the sinusoids at the metastasis/liver parenchyma interface. These TIMP-1-positive cells were in most cases adjacent to CD34-positive endothelial cells at the metastasis/liver parenchyma interface (see Figure 1I, L). No TIMP-1 hybridization signal was seen in the CD34-positive endothelial cells (see Figure 1J, K, L) or in CD68-positive cells (data not shown) in any of the samples tested, neither in primary colorectal cancer nor in the metastases.

Hepatic stellate cells, which are located within the Space of Disse of liver sinusoids, are normally activated during liver injury including metastasis to the liver [23]. Activation of hepatic stellate cells results in increased expression of various proteins. None of these proteins are, however, specific for activated hepatic stellate cells, and identification of activated hepatic stellate cells is therefore normally carried out by staining for α-SMA as well as morphological characterization [20,22–25]. As TIMP-1 mRNA in liver metastases with pushing growth pattern was found in α-SMA-positive cells located within the sinusoid, we consider these as activated hepatic stellate cells. This implies that in liver metastases with pushing growth pattern TIMP-1 protein is produced by hepatic stellate cells.

TIMP-1, PAI-1 and α-SMA in Activated Hepatic Stellate Cells In Vitro

In order to support the tentative identification of the TIMP-1-positive cells as hepatic stellate cells in metastases with pushing and replacement growth patterns we analyzed the presence of TIMP-1 and α-SMA in the immortalized hepatic stellate cell lines LX-1 and LX-2 [20] by Western blotting. We included PAI-1 since this protein show a similar expression pattern as TIMP-1 in liver metastases (Table 1). The cell lysates were subjected to temperature-induced phase-separation [26] in order to separate intracellular soluble proteins to the water-phase and enriching integral membrane proteins in the detergent-phase. TIMP-1 was found in the water-phase in both LX-1 and LX-2 cell lysates with a higher concentration in LX-1 compared to LX-2 cells (Figure 3). A comparison of the intensities of the TIMP-1 bands indicates that the amount of TIMP-1 in 9.4×10^5 LX-1 cells exceeds 20 ng (Figure 3). No TIMP-1 was detected in the detergent-phase, whereas the membrane bound uPAR as expected was enriched in the detergent-phase (data not shown). The majority of PAI-1 was found in the water-phases and only a weak band was present in the detergent-phase. On the cell surface PAI-1 is bound to uPA, which is cell surface located through binding to

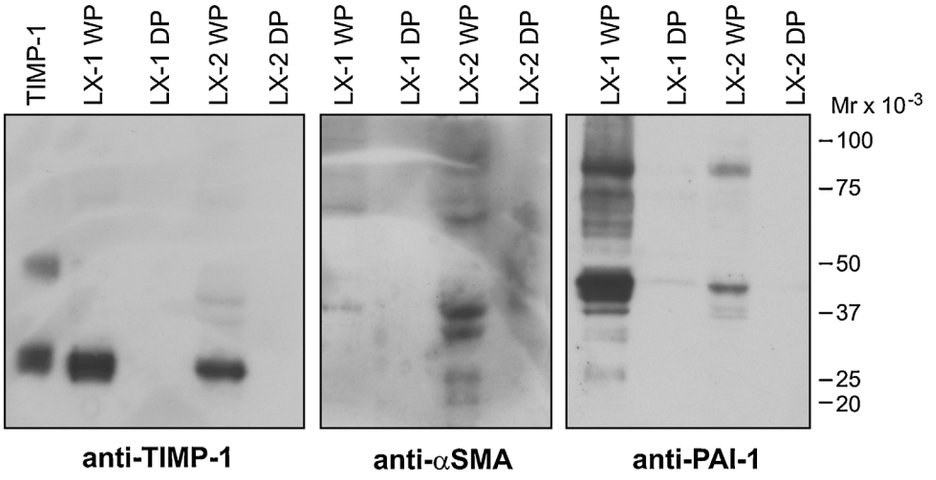

Figure 3. TIMP-1, α-SMA and PAI-1 in the immortalized hepatic stellate cells. Triton X-114 water-phases (WP) and detergent-phase (DP) extracts of either LX-1 or of LX-2 cells were prepared and loaded (each lane WP or DP from approximately 9.4×10^5 cells) on non-reduced SDS-PAGE gels, followed by Western blotting using 2 μg/ml of the following antibodies: mAb against TIMP-1, mAb against α-SMA and a pAb against PAI-1. In lane 1, 20 ng of purified recombinant TIMP-1 was applied as positive control. Electrophoretic mobility of standard proteins are indicated to the right.

its receptor uPAR. The proteins are internalized [27] and in the LX-1 and LX-2 cells the majority of PAI-1 is found in the water-phase. Judged from the apparent molecular weight, an uPA-PAI-1 complex is also present in LX-1 and LX-2 water-phases. A band with an apparent molecular weight of 42 kDa, which is the molecular weight of α-SMA, was detected in both water-phases. The additional bands visible in anti-α-SMA stained LX-2 water-phase and anti-PAI-1 stained LX-1 water-phase were absent when the primary antibody was omitted (Figure 3). The immunohistochemical localization of TIMP-1 was thus supported by the presence of TIMP-1 in the water-phase in lysed cultured activated hepatic stellate cells.

TIMP-1 and PAI-1 Double Immunofluorescence in Colorectal Liver Metastasis

The expression and localization of TIMP-1 in colorectal liver metastases are very similar to what we have described earlier for PAI-1, see Table 1 and Illemann et al. [8]. We therefore performed double immunofluorescence for TIMP-1 and PAI-1 on eight representative samples of colorectal liver metastasis from the cohort with paired primaries; four with a desmoplastic and four with a pushing growth pattern in order to determine if TIMP-1 and PAI-1 are localized in the same cells. In all four liver metastases with the desmoplastic growth pattern both TIMP-1 and PAI-1 are expressed by primarily myofibroblasts located in front of the cancer cells within the desmoplastic formation (Figure 4A–C). Most of the TIMP-1-positive myofibroblasts are also positive for PAI-1 but there are in general more PAI-1-positive cells. In the liver metastasis with a pushing growth pattern, TIMP-1-positive activated hepatic stellate cells are also positive for PAI-1 (see white arrows in Figure 4D–F). TIMP-1 and PAI-1 are also co-localized in some hepatocytes in both liver metastases with desmoplastic growth patterns (data not shown) and in liver metastasis with pushing growth pattern (see yellow arrows in Figure 4D, E, F). Expression of PAI-1 in hepatocytes is, however, more pronounced (see pink arrows in Figure 4E, F). TIMP-1-immunofluorescence was also observed in some cancer cells in all liver

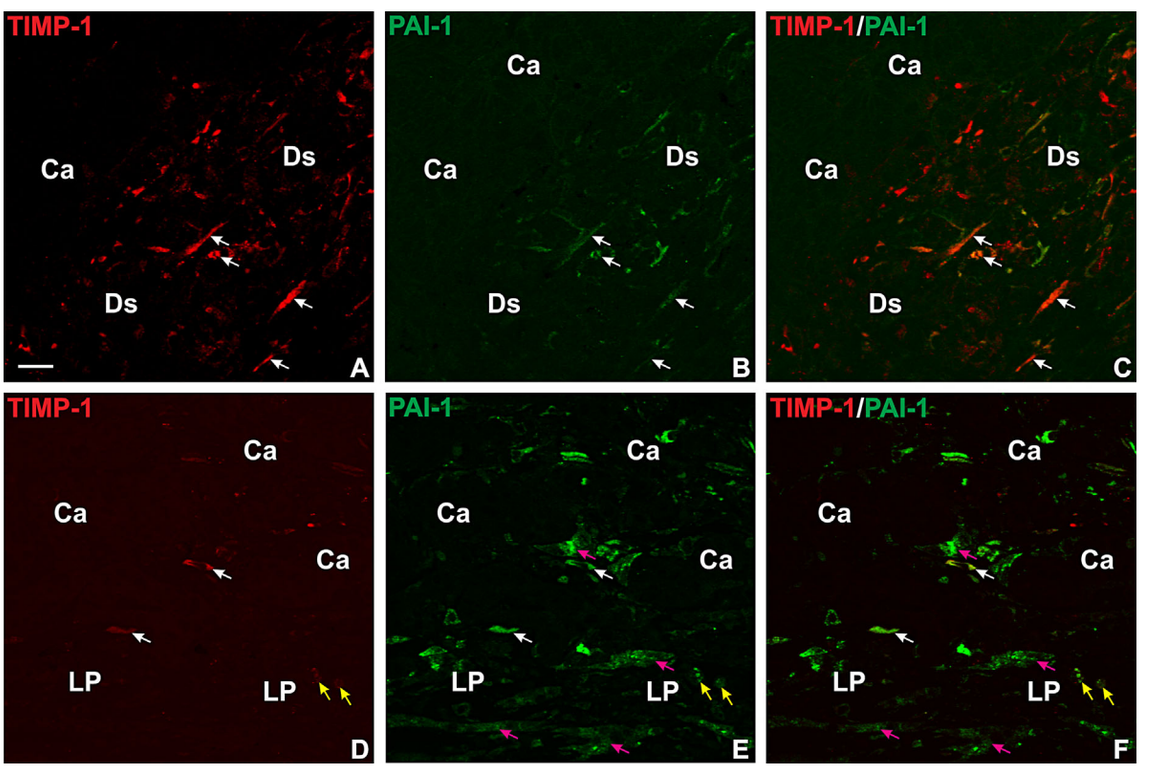

Figure 4. TIMP-1 and PAI-1 double immunofluorescence in liver metastases. A section from a liver metastasis with desmoplastic growth pattern (A–C) and a liver metastasis with pushing growth pattern (D–F) were processed for double immunofluorescence staining by incubation with a mAb against TIMP-1 together with a pAb against PAI-1. The TIMP-1 mAb was detected with Cy3-labeled goat-anti-mouse IgG (red signal in A, C, D, F) and the pAb against PAI-1 with FITC-labeled goat-anti-rabbit IgG (green signal in B, C, E, F). Co-localization of the two fluorophores is displayed in yellow (C, F). In the liver metastasis with desmoplastic growth pattern, co-localization of TIMP-1 and PAI-1 is found in myofibroblasts within the desmoplastic stroma formation (indicated with DS) (white arrows in A–C). In the liver metastasis with pushing growth pattern, TIMP-1 and PAI-1 co-localization is found in activated hepatic stellate cells (white arrows in D–F) and in some hepatocytes at the metastasis/liver parenchyma interface (indicated with LP) (yellow arrows in D–F). Note several hepatocytes are PAI-1 positive but negative for TIMP-1 (pink arrows in E, F). Bar in A, ~20 μm.

metastases analysed (primarily in the metastatic core, data not shown).

TIMP-1 and PAI-1 Co-Expression in Colorectal Liver Metastases

In order to reliably determine the TIMP-1-expression pattern in liver metastases with replacement growth pattern, we included liver metastases from another cohort where the matching primary tumors were not available. We included liver metastases with desmoplastic and pushing growth patterns from the same cohort to serve as a control and validate the finding from the first cohort.

Ten liver metastases of each growth pattern from the cohort without paired primaries were processed for TIMP-1 or PAI-1-immunohistochemistry. The expression patterns in metastases with desmoplastic and pushing growth patterns were identical to that seen in metastases from the English cohort (Figures, 2, 4 and 5 1A–D). In metastases with replacement growth pattern TIMP-1-immunoreactivity was primarily seen in spindle-shaped cells (presumably hepatic stellate cells) located in between the tumor glands at the metastasis/liver parenchyma interface (see black arrows in Figure 5E) as well as in some hepatocytes located in front of the metastatic cells (data not shown). The TIMP-1-positive hepatic stellate cells were on adjacent sections found positive for PAI-1 (see black arrows in Figure 5F). In addition, PAI-1-protein was found in some hepatocytes just at the metastasis/liver parenchyma interface (red arrows in Figure 5B, D, F). TIMP-1-immunoreactivity was also observed in fibroblast-like cells located in central parts of the metastasis in areas with fibrosis and/or necrosis (data not shown), and in some cancer cells scattered throughout the tumor tissue (primarily in the metastatic core, data not shown).

Secondary Sites of TIMP-1-Expression in Colorectal Liver Metastases

In liver metastases with either desmoplastic or pushing growth pattern TIMP-1 mRNA and protein were in addition found in fibroblast-like cells (most likely myofibroblasts) in the muscular part of large hepatic arteries, in endothelial cells veins (both hepatic veins and central veins), in spindle-shaped cells located in areas of bile duct proliferation (see Figure 6). As TIMP-1-expression at these sites often was found distant to the site of metastasis, it may not be related to cancer but most likely to pathological changes in the liver in general. In normal appearing liver tissue, no TIMP-1-expression was observed (data not shown).

MMP-2 In Situ Hybridization in Primary Colorectal Cancer and Its Matching Liver Metastasis

It has been reported that colorectal cancer patients with high metastatic burden have elevated levels of type IV collagen fragments [28]. Such fragments are generated by MMP-2 and MMP-9, and both these enzymes can be inhibited by TIMP-1 [7]. Since we have previously shown that MMP-9 is not up-regulated in colorectal cancer liver metastases [9] we decided to focus on MMP-2 and analyze a subset of the liver metastases for MMP-2-expression. Therefore six representative cases of paired samples of primary colorectal cancer and their matching liver metastases, of which three had liver metastases with a desmoplastic growth pattern and three had a pushing growth pattern were processed for in situ hybridization using an antisense MMP-2 ^{35}S-UTP mRNA, which has been previously employed [14,18]. In all six primary colorectal cancers, MMP-2 mRNA was found in numerous fibroblast-like cells (presumably myofibroblasts) located in both the stroma in front of the cancer as well as in the submucosa (see Figure 7A, D) similar to previous reports [12,18,29]. In the colonic mucosa, which appeared normal, no MMP-2 mRNA was detected (data not shown). MMP-2 mRNA was not identified in malignant cells and no in situ hybridization signal was seen using the corresponding ^{35}S-UTP mRNA sense probe (data not shown). In the three liver metastases with a desmoplastic growth pattern, MMP-2 mRNA was confined to fibroblast-like cells (presumably myofibroblasts) located within the desmoplastic zone and in cells in between the cancer glands (see Figure 7B, E). MMP-2 mRNA expression was not detected in cancer cells. No MMP-2 mRNA was detected either at the front of the metastases or in stromal cells located in between the metastatic cancer glands in the three investigated liver metastases with a pushing growth pattern, (see Figure 7C, F). No expression of MMP-2 mRNA was seen at any of the secondary sites, which showed expression of TIMP-1 (see above and Figure 6).

DISCUSSION

We have determined the cellular localization of TIMP-1 in liver metastases from two cohorts of colorectal cancer patients, one including the matching primary tumors. TIMP-1 mRNA and protein was localized to activated α-SMA-positive myofibroblasts in primary colorectal cancer and in liver metastases with desmoplastic growth pattern. TIMP-1 was highly expressed and often found in cells adjacent to CD34-positive endothelial cells, which suggests that TIMP-1 was expressed by pericytes, a cell type that covers mature vessel walls as well as being involved in tumor angiogenesis and metastasis [30]. In liver metastases with pushing or replacement growth patterns, TIMP-1 mRNA and protein were seen in activated hepatic stellate cells located at the metastasis/liver parenchyma interface. Hepatic stellate cells are activated in response to injury of the liver [23]. In addition, we have shown that MMP-2 mRNA is highly up-regulated in primary colorectal cancer and in liver metastases with desmoplastic

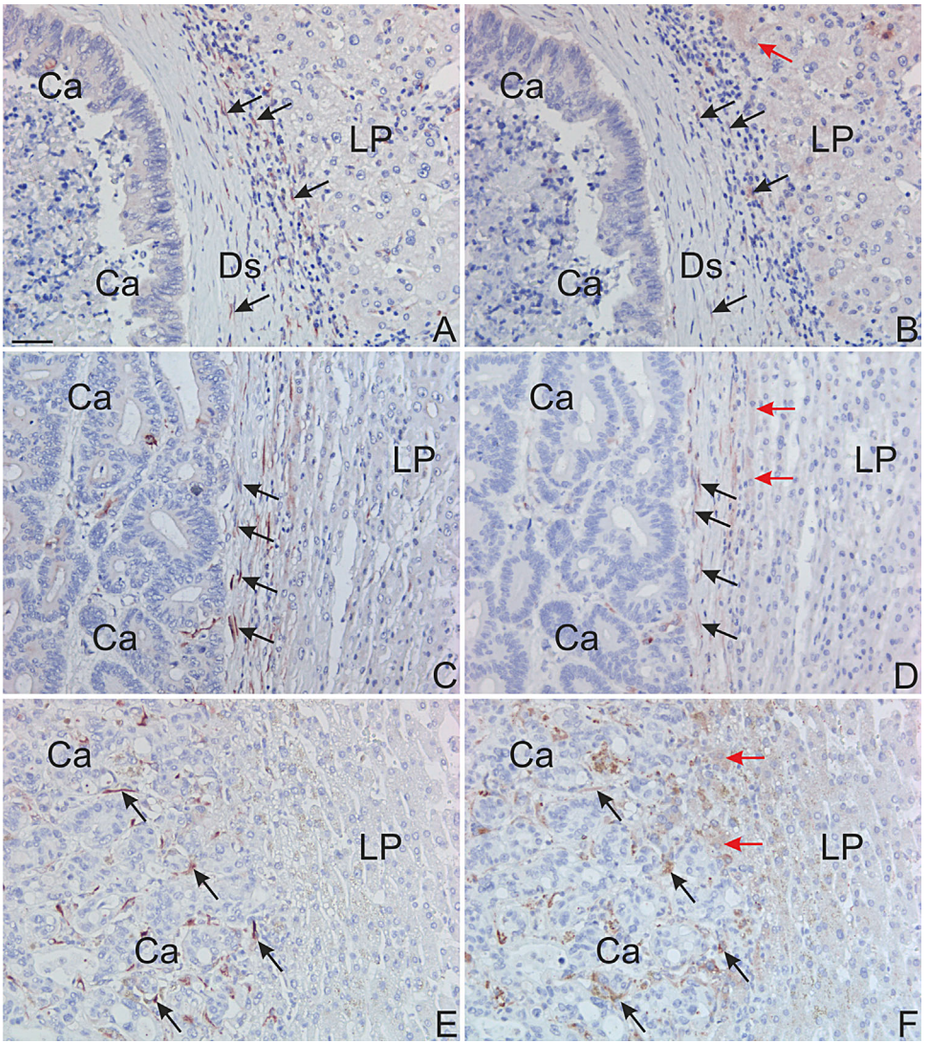

Figure 5. TIMP-1 and PAI-1 immunohistochemistry in liver metastasis from a different patient cohort. Neighboring section from a liver metastasis with desmoplastic growth pattern (A, B), a liver metastasis with pushing growth pattern (C, D), and a liver metastasis with replacement growth pattern (E, F) were processed for immunoperoxidase staining using a mAb against TIMP-1 (A, C, D) or a pAb against PAI-1 (B, D, F). The immunoperoxidase stainings are developed with NovaRed. TIMP-1 and PAI-1-immunoreactivity are seen co-expressed in primarily myofibroblasts in the liver metastasis with desmoplastic growth pattern and are within the desmoplasia (black arrows in A and B). In the liver metastases with pushing and replacement growth patterns, TIMP-1 and PAI-1 are co-expressed in activated hepatic stellate cells located in between the tumor glands at the metastasis/liver parenchyma interface (black arrows in C–F). PAI-1-immunoreactivity is also seen in hepatocytes at the front of the metastases (red arrows in B, D, F). Bar in A, ~50 μm.

growth pattern and presumable expressed by cells that are also TIMP-1-positive. In liver metastases with pushing growth pattern no MMP-2 mRNA was found.

TIMP-1-expression in α-SMA-positive myofibroblasts at the invasive front of the primary colorectal cancer as well as in some few cancer cells have previously been described [12,14]. We do, nevertheless, add new information about the localization of TIMP-1 in primary colorectal cancer, as we have found that around 50% of the TIMP-1-positive cells are pericytes located adjacent to CD34-positive endothelial cells.

We have identified myofibroblast, pericytes and hepatic stellate cells as the main sites of synthesis of TIMP-1 in liver metastases. As expected the TIMP-1 protein is localized in the same cells as the TIMP-1 mRNA and the TIMP-1-immunoreactivity was confined to the cytoplasm. Interestingly, TIMP-1 mRNA seems in general to be expressed in more cells and with a higher level in the liver metastases compared to the expression in the primary tumor. This is in agreement with the finding that significantly higher levels of TIMP-1 are found in plasma from patients with metastatic colorectal cancer compared to patients with non-metastatic disease [11]. With

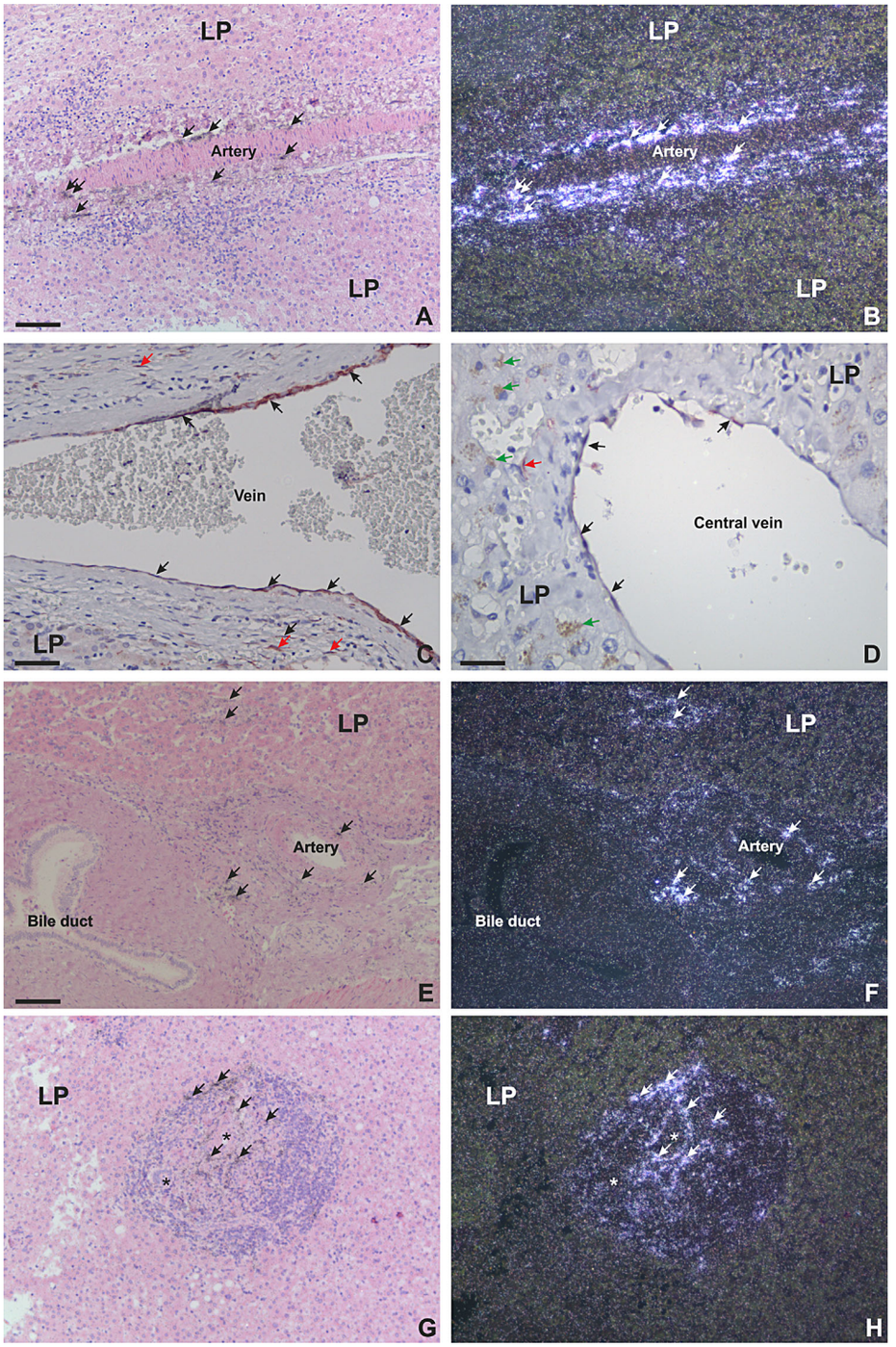

Figure 6. *In situ* hybridization and immunohistochemistry for TIMP-1 mRNA and protein: secondary locations of TIMP-1 in colorectal liver metastases. Sections of colorectal liver metastases were processed for either *in situ* hybridization using TIMP-1 mRNA antisense probes (A–B, E–H) or immunohistochemistry using a mAb against TIMP-1 (C–D). The TIMP-1 mRNA probe is visualized as black silver grains in bright-field illumination (A, E, G) and white spots in dark-field illumination (B, F, H). The TIMP-1-immunoperoxidase stainings are developed with NovaRed (C–D). TIMP-1 mRNA is found in fibroblast-like cells within structure of large hepatic artery (arrows in A–B, E–F), in vessels near large bile ducts (arrows in E–F) and in spindle shape-like cells in areas with bile duct proliferations (arrows in G–H). TIMP-1-immunoreactivity was found in endothelial cells in large hepatic veins and in central veins (black arrows in C—D) as well as in fibroblast-like cells within the wall of the veins (red arrows in C). Green arrows in D show brown coloring in hepatocytes, which is accumulation of bile due to interhepatic cholestatis. Bars, ~100 μm (A, B, E–H), ~50 μm (C), and ~25 μm (D).

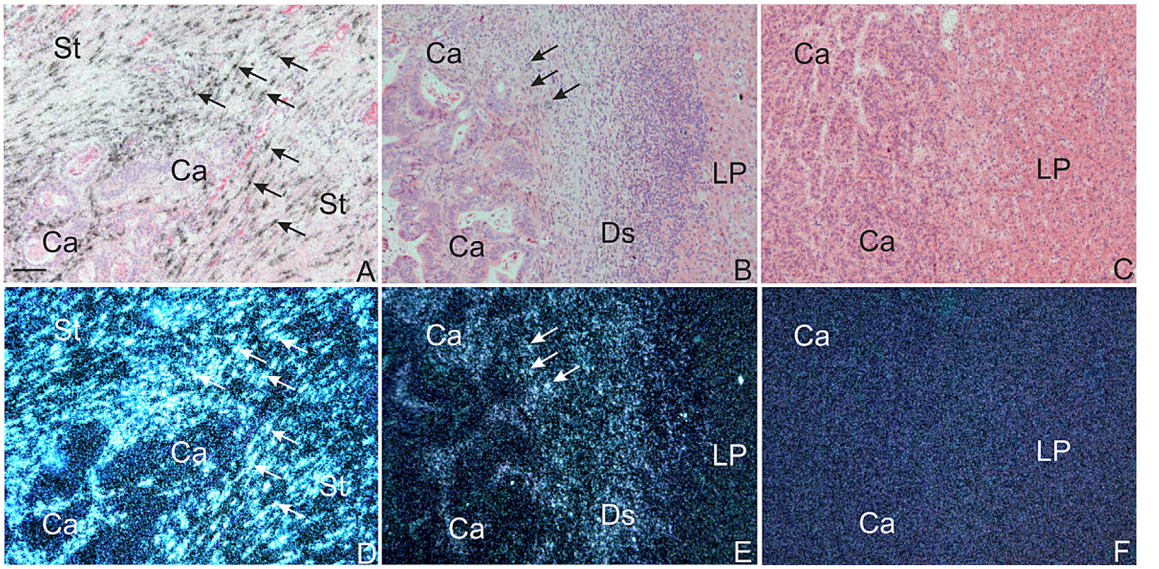

Figure 7. *In situ* hybridization for MMP-2 mRNA in colon adenocarcinoma and its liver metastases. Sections from a colon adenocarcinoma (Left Column: A, D), its liver metastasis with desmoplastic growth (Centre Column: B, E), and a liver metastasis with pushing growth pattern (Right Column: C, F,) were processed for in situ hybridization using MMP-2 mRNA antisense probes. The MMP-2 mRNA probe is visualized as black silver grains in bright-field illumination (A–C) and white spots in dark-field illumination (D–F). In both the colon adenocarcinoma and the liver metastasis with desmoplastic growth, MMP-2 mRNA is found expressed by stromal fibroblast-like cells at the tumor edge as well as in between the cancer glands (arrows in A, B, D, E). No MMP-2 mRNA signal is detected in the liver metastases with pushing growth pattern (C and F). Bar, ~100 μm (A–F).

regards to TIMP-1-expression in the colorectal cancer liver metastases, our data are in general compatible with a study by Zeng et al., where TIMP-1 mRNA by in situ hybridization was found in spindle-shaped stromal cells [15].

The primary function for TIMP-1 is to inhibit the MMPs. In primary colon cancer several MMPs (including MMP-2 and MMP-11) are expressed by fibroblasts-like cells (most likely myofibroblasts) similar to TIMP-1, whereas MMP-9 is primarily expressed by macrophages and neutrophils [9,12–15,18,29,31,32]. Since TIMP-1, as well as these MMPs, are secreted from the cells, inhibition of an MMP by TIMP-1 is independent of the cellular location.

Little is known about the expression of MMPs in liver metastases. MMP-9 was primarily found in neutrophils and only in few cases in macrophages in liver metastases [9]. We here demonstrate MMP-2 mRNA to be expressed by fibroblast-like cells (presumably myofibroblasts) in the stroma surrounding the cancer glands of colon adenocarcinomas and in liver metastases with a desmoplastic growth pattern, whereas no MMP-2 mRNA was present in metastases with a pushing growth pattern. Previous studies have also localized MMP-2 mRNA to fibroblasts within the desmoplastic formation of colon cancer liver metastases and in hepatocellular carcinomas with fibrotic encapsulation [33–35]. TIMP-1 could therefore function as an inhibitor of MMPs in both primary colorectal cancer and liver metastases with a desmoplastic growth pattern. This would, however, not be the main function in liver metastases with pushing growth pattern, as we did not detect any MMP-2 mRNA and there is no expression of MMP-9 [9]. Interestingly, another protease active in tissue remodeling, uPA is only up-regulated in stromal cells in liver metastases with desmoplastic growth pattern [8], see Table 1. These findings indicate that cancer cell expansion/invasion into the surrounding liver might be growth pattern specific.

Three different histological growth patterns of tumors have earlier been described in hepatocellular carcinoma [36]. These are referred to as encapsulated, sinusoidal, and replacement growth patterns. In the encapsulated growth, which is identical to the desmoplastic growth pattern in liver metastases, the liver cells at the desmoplasia/liver parenchyma interface collapse and seemingly disappear as the tumor expands [36]. It is also suggested in this study that the reticulin fibers, which are made up of different types of collagens, are left behind, generating a collagen-rich fibrous capsule [36,37]. In the sinusoidal growth pattern, similar to the pushing growth pattern, the tumor cells grow in an infiltrating manner in the sinusoids at the metastasis/liver parenchyma interface, and thereby compress the liver cell cord, and gradually the cancer cells take over the liver cell cord [36]. In the replacement growth pattern, the tumor cells are replacing the hepatocytes along the liver cell cord, and the tumor cells may adhere to one another forming nests in an organoid arrangement [36]. It is very likely that the

growth patterns of liver metastasis from colorectal cancer use similar invasive mechanisms as those described in hepatocellular carcinoma. Therefore we have earlier suggested that metastatic cancer cells in the liver metastases with the desmoplastic growth pattern are found behind a barrier of collagens, and recruitment of stromal cells for the secretion of proteases is essential for the ability to grow and invade [8]. In contrast, liver metastases with the pushing growth pattern may invade the liver using a different, perhaps protease independent mechanism (as no protease expression so far have been found) and may even invade the liver through the cavities of the sinusoids [8].

MMP-independent activity of TIMP-1 is found in stimulation of cell proliferation, angiogenesis and apoptosis, in which TIMP-1 is believed to have an anti-apoptotic effect [38,39]. Using an experimental liver metastasis model it has been shown that host derived expression of TIMP-1 can promote formation of liver metastasis [40]. Interestingly, we found TIMP-1-expression in liver host cells like myofibroblasts, hepatic stellate cells and hepatocytes and the expression level was higher in the liver metastases than in the primary tumors (Figures, 2, 4, 5 1). The expression of TIMP-1 was higher in host cells close to the cancer cells in the liver metastases, independent of growth pattern (Figure 5), indicating that cancer cells can affect the expression level of TIMP-1 in the different host cells. TIMP-1 has also been reported to be involved in angiogenesis with both pro- and anti-angiogenic effects [38]. This can indirectly be exerted through inhibition of MMPs by TIMP-1. For instance, by using a 3D-dimensional angiogenesis assay fibroblast derived TIMP-1 was shown to increase vessel assembly [41]. It was further demonstrated that TIMP-1 can promote angiogenesis indirectly by blocking MMP-2/9 mediated generation of tumstatin, an anti-angiogenic fragment of type IV collagen degradation [41]. This fits well with our study, as we have found that MMP-2 mRNA is only expressed in the liver metastases with desmoplastic growth pattern. We have not found MMP-2 mRNA in liver metastases with pushing growth pattern, which has the highest angiogenic activity of the three metastatic growth patterns [1,2,4]. In another study, in vivo inhibition of TIMP-1 by the use of a specific blocking antibody has shown to increase fibrovascular invasion thereby increasing angiogenesis [42].

The inhibitor of uPA, PAI-1 is expressed by α-SMA-positive cells in both primary colorectal adenocarcinomas and all liver metastases regardless of growth pattern [8]. In the primary tumor as wells as in liver metastases with the desmoplastic growth pattern, PAI-1 is expressed by α-SMA-positive myofibroblasts, whereas the PAI-1-positive cells in the liver metastases with pushing growth patterns are α-SMA-positive cells, most likely activated hepatic stellate cells, located at the periphery of the metastases and associated with sinusoids [8]. We have, in this study, also shown that the expression patterns of TIMP-1 and PAI-1 are almost identical as they are partly expressed by same cells. As MMPs, as well as the plasminogen activation system, are more or less absent from liver metastases with a pushing growth pattern [8], it is tempting to speculate that the two protease inhibitors, TIMP-1 and PAI-1, carry out functions not dependent on inhibition of proteolysis but related to cancer progression in these liver metastases. This is supported by the fact that both circulating TIMP-1 and PAI-1 are strong prognostic markers with high levels correlating to poor prognosis [10,11,43–46].

The prognostic value of TIMP-1 in colorectal cancer is consistent with the reported anti-apoptopic and pro-angiogenic activity of TIMP-1 [38,39]. The anti-apoptopic activity of TIMP-1 can be achieved through different mechanisms, either dependent or independent of inhibition of MMPs. In addition TIMP-1 binding to the cell surface receptor CD63 inhibits apoptosis and cell growth [38,39]. The pro-angiogenic activity, quantified as the level of endothelial cell proliferation, is higher in liver metastases with a pushing growth pattern than in those with a desmoplastic or replacement growth patterns [1–3]. Interestingly, colorectal cancer patients with liver metastases with a pushing growth pattern have a poorer prognosis than those with the two other growth patterns [4]. The plasma concentration of TIMP-1 is highest in patients with metastatic disease [11] which is consistent with the higher expression of TIMP-1 in liver metastases compared to the primary tumor that we find (see Figure 1, 2, and 4). Due to the intense cytoplasmic staining we were not able to detect membrane staining of TIMP-1 and may of that reason not be able to identify CD63-bound TIMP-1.

In conclusion, TIMP-1 is expressed by different stromal cell types in colorectal cancer liver metastases with different growth patterns. In metastases with the desmoplastic growth pattern, the TIMP-1-expression pattern indicates dual functions. At the metastasis periphery, TIMP-1 in myofibroblasts could have MMP inhibitory activity. TIMP-1 in pericytes adjacent to CD34-positive endothelial cells could be involved in tumor angiogenesis [30]. In liver metastases with the pushing growth pattern, TIMP-1 was expressed by activated hepatic stellate cells located adjacent to CD34-positive endothelial cells, suggesting a function in tumor induced angiogenesis.

ACKNOWLEDGMENTS

We thank Scott L. Friedman for the two cell lines LX-1 and LX-2. We thank Öznur Turan and Lene Kjaer Callesen for excellent technical assistance, and John Post for photographic assistance. We also thank our colleagues and associated members of the Liver

Metastasis Research Network (www.lmrn.org) for inspiring discussions.

REFERENCES

1. Vermeulen PB, Colpaert C, Salgado R, et al. Liver metastases from colorectal adenocarcinomas grow in three patterns with different angiogenesis and desmoplasia. J Pathol 2001;195: 336–342.
2. Stessels F, Van den Eynden G, Van der Auwera I, et al. Breast adenocarcinoma liver metastases, in contrast to colorectal cancer liver metastases, display a non-angiogenic growth pattern that preserves the stroma and lacks hypoxia. Br J Cancer 2004;90:1429–1436.
3. Eefsen RL, Van den Eynden GG, Høyer-Hansen G, et al. Histopathological growth pattern, proteolysis and angiogenesis in chemonaive patients resected for multiple colorectal liver metastases. J Oncol 2012;2012:907971.
4. Van den Eynden GG, Bird NC, Majeed AW, et al. The histological growth pattern of colorectal cancer liver metastases has prognostic value. Clin Exp Metastasis 2012;29:541–549.
5. Hanahan D, Weinberg RA. Hallmarks of cancer: The next generation. Cell 2011;144:646–674.
6. Danø K, Rømer J, Nielsen BS, et al. Cancer invasion and tissue remodeling–cooperation of protease systems and cell types. APMIS 1999;107:120–127.
7. Egeblad M, Werb Z. New functions for the matrix metalloproteinases in cancer progression. Nat Rev Cancer 2002; 2:163–176.
8. Illemann M, Bird N, Majeed A, et al. Two distinct expression patterns of urokinase, urokinase receptor and plasminogen activator inhibitor-1 in colon cancer liver metastases. Int J Cancer 2009;124:1860–1870.
9. Illemann M, Bird N, Majeed A, et al. MMP-9 is differentially expressed in primary human colorectal adenocarcinomas and their metastases. Mol Cancer Res 2006;4:293–302.
10. Holten-Andersen MN, Murphy G, Nielsen HJ, et al. Quantitation of TIMP-1 in plasma of healthy blood donors and patients with advanced cancer. Br J Cancer 1999;80:495–503.
11. Holten-Andersen MN, Stephens RW, Nielsen HJ, et al. High preoperative plasma tissue inhibitor of metalloproteinase-1 levels are associated with short survival of patients with colorectal cancer. Clin Cancer Res 2000;6:4292–4299.
12. Newell KJ, Witty JP, Rodgers WH, Matrisian LM. Expression and localization of matrix-degrading metalloproteinases during colorectal tumorigenesis. Mol Carcinog 1994;10: 199–206.
13. Zeng ZS, Cohen AM, Zhang ZF, Stetler-Stevenson W, Guillem JG. Elevated tissue inhibitor of metalloproteinase 1 RNA in colorectal cancer stroma correlates with lymph node and distant metastases. Clin Cancer Res 1995;1:899–906.
14. Holten-Andersen MN, Hansen U, Brünner N, Nielsen HJ, Illemann M, Nielsen BS. Localization of tissue inhibitor of metalloproteinases 1 (TIMP-1) in human colorectal adenoma and adenocarcinoma. Int J Cancer 2005;113:198–206.
15. Zeng ZS, Guillem JG. Distinct pattern of matrix metalloproteinase 9 and tissue inhibitor of metalloproteinase 1 mRNA expression in human colorectal cancer and liver metastases. Br J Cancer 1995;72:575–582.
16. Tot T. Cytokeratins 20 and 7 as biomarkers: Usefulness in discriminating primary from metastatic adenocarcinoma. Eur J Cancer 2002;38:758–763.
17. Offersen BV, Nielsen BS, Høyer-Hansen G, et al. The myofibroblast is the predominant plasminogen activator inhibitor-1-expressing cell type in human breast carcinomas. Am J Pathol 2003;163:1887–1899.
18. Pyke C, Ralfkiær E, Tryggvason K, Danø K. Messenger RNA for two type IV collagenases is located in stromal cells in human colon cancer. Am J Pathol 1993;142:359–365.
19. Dickinson ME, Bearman G, Tilie S, Lansford R, Fraser SE. Multispectral imaging and linear unmixing add a whole new dimension to laser scanning fluorescence microscopy. Biotechniques 2001;31:1272–1278.
20. Xu L, Hui AY, Albanis E, et al. Human hepatic stellate cell lines, LX-1 and LX-2: New tools for analysis of hepatic fibrosis. Gut 2005;54:142–151.
21. Høyer-Hansen G, Rønne E, Solberg H, et al. Urokinase plasminogen activator cleaves its cell surface receptor releasing the ligand-binding domain. J Biol Chem 1992;267:18224–18229.
22. Van den Eynden GG, Majeed AW, Illemann M, et al. The multifaceted role of the microenvironment in liver metastasis: Biology and clinical implications. Cancer Res 2013;73:2031–2043.
23. Friedman SL. Mechanisms of hepatic fibrogenesis. Gastroenterology 2008;134:1655–1669.
24. Olaso E, Salado C, Egilegor E, et al. Proangiogenic role of tumor-activated hepatic stellate cells in experimental melanoma metastasis. Hepatology 2003;37:674–685.
25. Castilho-Fernandes A, de Almeida DC, Fontes AM, et al. Human hepatic stellate cell line (LX-2) exhibits characteristics of bone marrow-derived mesenchymal stem cells. Exp Mol Pathol 2011;91:664–672.
26. Bordier C. Phase separation of integral membrane proteins in Triton X-114 solution. J Biol Chem 1981;256:1604–1607.
27. Olson D, Pöllänen J, Høyer-Hansen G, et al. Internalization of the urokinase-plasminogen activator inhibitor type-1 complex is mediated by the urokinase receptor. J Biol Chem 1992;267:9129–9133.
28. Nyström H, Naredi P, Hafström L, Sund M. Type IV collagen as a tumour marker for colorectal liver metastases. Eur J Surg Oncol 2011;37:611–617.
29. Poulsom R, Pignatelli M, Stetler-Stevenson WG, et al. Stromal expression of 72 kda type IV collagenase (MMP-2) and TIMP-2 mRNAs in colorectal neoplasia. Am J Pathol 1992;141:389–396.
30. Raza A, Franklin MJ, Dudek AZ. Pericytes and vessel maturation during tumor angiogenesis and metastasis. Am J Hematol 2010;85:593–598.
31. Zeng ZS, Huang Y, Cohen AM, Guillem JG. Prediction of colorectal cancer relapse and survival via tissue RNA levels of matrix metalloproteinase-9. J Clin Oncol 1996;14:3133–3140.
32. Nielsen BS, Timshel S, Kjeldsen L, et al. 92 kDa type IV collagenase (MMP-9) is expressed in neutrophils and macrophages but not in malignant epithelial cells in human colon cancer. Int J Cancer 1996;65:57–62.
33. Lunevicius R, Nakanishi H, Ito S, et al. Clinicopathological significance of fibrotic capsule formation around liver metastasis from colorectal cancer. J Cancer Res Clin Oncol 2001;127:193–199.
34. Musso O, Théret N, Campion JP, et al. In situ detection of matrix metalloproteinase-2 (MMP2) and the metalloproteinase inhibitor TIMP2 transcripts in human primary hepatocellular carcinoma and in liver metastasis. J Hepatol 1997; 26:593–605.
35. Théret N, Musso O, Turlin B, et al. Increased extracellular matrix remodeling is associated with tumor progression in human hepatocellular carcinomas. Hepatology 2001;34:82–88.
36. Nakashima T, Kojiro M, Kawano Y, et al. Histologic growth-pattern of hepatocellular-carcinoma - relationship to orcein (Hepatitis-B surface antigen)-positive cells in cancer-tissue. Hum Pathol 1982;13:563–568.
37. Ushiki T. Collagen fibers, reticular fibers and elastic fibers. A comprehensive understanding from a morphological viewpoint. Arch Histol Cytol 2002;65:109–126.
38. Møller Sørensen N, Sørensen IV, Ornbjerg WS, et al. Biology and potential clinical implications of tissue inhibitor of metalloproteinases-1 in colorectal cancer treatment. Scand J Gastroenterol 2008;43:774–786.

39. Stetler-Stevenson WG. Tissue inhibitors of metalloproteinases in cell signaling: Metalloproteinase-independent biological activities. Sci Signal 2008;1:re6.
40. Kopitz C, Gerg M, Bandapalli OR, et al. Tissue inhibitor of metalloproteinases-1 promotes liver metastasis by induction of hepatocyte growth factor signaling. Cancer Res 2007;67:8615–8623.
41. Liu H, Chen B, Lilly B. Fibroblasts potentiate blood vessel formation partially through secreted factor TIMP-1. Angiogenesis 2008;11:223–234.
42. Reed MJ, Koike T, Sadoun E, Sage EH, Puolakkainen P. Inhibition of TIMP1 enhances angiogenesis in vivo and cell migration in vitro. Microvasc Res 2003;65:9–17.
43. Nielsen HJ, Pappot H, Christensen IJ, et al. Association between plasma concentrations of plasminogen activator inhibitor-1 and survival in patients with colorectal cancer. BMJ 1998;316:829–830.
44. Herszényi L, Farinati F, Cardin R, et al. Tumor marker utility and prognostic relevance of cathepsin B, cathepsin L, urokinase-type plasminogen activator, plasminogen activator inhibitor type-1, CEA and CA 19–9 in colorectal cancer. BMC Cancer 2008;8:194.
45. Langenskiöld M, Holmdahl L, Angenete E, Falk P, Nordgren S, Ivarsson ML. Differential prognostic impact of uPA and PAI-1 in colon and rectal cancer. Tumour Biol 2009;30:210–220.
46. Yamada Y, Arao T, Matsumoto K, et al. Plasma concentrations of VCAM-1 and PAI-1: A predictive biomarker for post-operative recurrence in colorectal cancer. Cancer Sci 2010;101:1886–1890.